Carbohydrate Polymers 89 (2012) 899–905

Contents lists available at SciVerse ScienceDirect

Carbohydrate Polymers

journal homepage: www.elsevier.com/locate/carbpol

Interactions of cellulose-based comb polyelectrolyte with oppositely charged surfactant dodecyl-trimethylammonium bromide

Hong Pan[a,b], Pei-Yao Chen[a], Hai-Xue Liu[b], Yu Chen[a], Yu-ping Wei[a], Ming-Jie Zhang[a], Fa Cheng[a,*]

[a] Department of Chemistry, School of Science, Tianjin University, Tianjin 300072, PR China
[b] Department of Basic Science, Tianjin Agricultural College, Tianjin 300384, PR China

ARTICLE INFO

Article history:
Received 15 March 2012
Received in revised form 4 April 2012
Accepted 10 April 2012
Available online 21 April 2012

Keywords:
Interaction
Cellulose
Comb polyelectrolyte
Atom transfer radical polymerization

ABSTRACT

A comb ethyl cellulose-g-sodium polyacrylate (EC-g-SPA) was synthesized by atom transfer radical polymerization. The amphiphilic properties of the EC-g-SPA were determined by surface tension measurements. The interactions between EC-g-SPA and the cationic surfactant dodecyl-trimethylammonium bromide (C_{12}TAB) were investigated by surface tension, turbidity, dynamic light scattering and transmission electron microscopy (TEM). The results revealed that the critical aggregate concentration (CAC) of the complexes was 0.8 mM. When the C_{12}TAB concentration was lower than the CAC, the hydrodynamic diameter (D_h) of the complexes decreased as the surfactant concentration was increased. As the C_{12}TAB concentration was increased above the CAC, the D_h initially increased slightly, followed by a sharp decrease. The changes in the sizes and shapes of the aggregates were studied by TEM. The interactions between two species and the structure of the EC-g-SPA/C_{12}TAB complexes were also discussed.

1. Introduction

Interactions between polyelectrolytes and oppositely charged surfactants have attracted considerable interest due to their wide industrial applications in areas such as drug vehicles and home and personal care products (Goddard & Ananthapadmanabahn, 1993; Jönsson, Lindman, Holmberg, & Kronberg, 1998). Ionic surfactants can aggregate into micelle-like structures in the vicinity of oppositely charged polyions, and they can form tightly bound complexes at a defined concentration, known as the critical aggregation concentration (CAC) which is usually a few orders of magnitude lower than the critical micelle concentration (CMC) of the free surfactant (Penfold et al., 2007). The formation of polyelectrolyte/surfactant complexes is driven by electrostatic interactions between the surfactant head groups and the polyelectrolyte and by hydrophobic interactions between the hydrophobic backbones of the polyelectrolyte and the alkyl chains of the surfactant (Fundin, Hansson, Brown, & Lidegran, 1997; Penfold et al., 2007; Wang & Tam, 2002).

There has been a great deal of experimental and theoretical work done to determine the bulk properties of the neutral polymer/surfactant systems (Hansson & Almgren, 1994; Li, Lin, Cai, Scriven, & Davis, 1995), which are often referred to as "weakly interacting" systems (Goddard, 1986, 2002). In addition, the interfacial properties for these systems, which involve surface adsorption and surface tension behavior, have been well established (Jones, 1967). However, there are confusing results (Taylor et al., 2007) for systems of oppositely charged polyelectrolytes and surfactants, which are called strongly interacting systems. For example, surface tension profiles for sodium poly(styrene sulfonate) (PSS)/trimethylammonium bromide (C_{12}TAB) complexes (Taylor & Thomas, 2002a, 2002b; Taylor, Thomas, & Li, 2003) are quite different from those for sodium dodecyl sulfate (SDS)/poly(dimethyldiallylammonium chloride) (poly DMDAAC) complexes (Staples, Tuchker, Penfold, Warren, & Thomas, 2002; Staples, Tuchker, Penfold, Warren, Thomas, & Taylor, 2002). Macroscopic model of the surface tension of polymer/surfactant systems, which cover both weakly interacting and strongly interacting systems, has been proposed by Bell, Breward, Howell, Penfold, and Thomas (2007). But this model is aimed at systems such as SDS/PEO, SDS/PVP, SDS/polyDMDAAC and PSS/C_{12}TAB. The surface tension profiles for strongly interacting systems are influenced by the charge density, hydrophobicity and the topological structure of the polyelectrolyte. Understanding the surface tension behavior of amphiphilic polyelectrolyte/surfactant systems is less than straightforward.

Cellulose-based polyelectrolytes that interact with surfactants are the focus of commercial cellulose products, such as cationic cellulose (Lee & Moroi, 2004; Miyake & Kakizawa, 2002; Rodríguez, Alvarez-Lorenzo, & Concheiro, 2003; Svensson, Sjöström, Scheel, & Piculell, 2003) and anionic cellulose (Silvério & Okano, 2004; Trabelsi, Raspaud, & Langevin, 2007; Wu, Du, et al., 2009; Wu, Shangguan, et al., 2009). These cellulose-based polyelectrolytes are

* Corresponding author. Tel.: +86 22 27403475; fax: +86 22 27403475.
E-mail address: chengfa@tju.edu.cn (F. Cheng).

0144-8617/$ – see front matter © 2012 Elsevier Ltd. All rights reserved.
http://dx.doi.org/10.1016/j.carbpol.2012.04.032

linear and hydrophilic. Interest in molecular brushes arises from their compact branched structures and their persistent cylindrical shapes that confer many novel properties (Cui et al., 2006; Pakula et al., 2006; Zhang, Estournès, Bietsch, & Müller, 2004), such as interesting associative behavior in bulk solution and unique characteristics at interfaces (Varga, Mészáros, Makuška, Claesson, & Gilányi, 2009). The amphiphilic nature and the comb structure of polyelectrolytes will affect the surface tension behaviors of polyelectrolyte/surfactant systems. There have been a few studies on the complexes between comb polymers with nonionic hydrophilic side chains and surfactants (Middleton, English, Williams, & Broze, 2005). But to the best of our knowledge, the interactions between an amphiphilic cellulose-based polyelectrolyte and an oppositely charged surfactant and the interfacial properties of this system have not yet been reported.

In this paper, a comb amphiphilic polyelectrolyte ethyl cellulose-g-sodium polyacrylate (EC-g-SPA) was synthesized by atom transfer radical polymerization (ATRP). The amphiphilic properties of the comb polyelectrolyte EC-g-SPA were determined by surface tension measurements. The interactions between EC-g-SPA and the cationic surfactant dodecyl-trimethylammonium bromide (C_{12}TAB) were investigated by surface tension, turbidity, dynamic light scattering (DLS) and transmission electron microscopy (TEM). The CAC was also estimated by surface tension and DLS. The sizes and structures of the aggregates formed in the mixed system were studied by DLS and TEM. The interactions and the structure of the EC-g-SPA/C_{12}TAB complexes were also discussed. It is hoped that this work can provide a better understanding of the effect of amphiphilic structure (of EC-g-SPA) on the interactions between EC-g-SPA and C_{12}TAB and the interfacial properties of the present complexes system.

2. Experimental

2.1. Materials

The ethyl cellulose (EC, M_w = 46,367 g/mol, M_w/M_n = 1.967), with a degree of ethyl substitution of 2.44 (Luzhou Chemical Engineering Plant, Luzhou, China), was dried at 80 °C for 48 h under vacuum before use. The N,N,N′,N″,N″-pentamethyldiethylenetriamine (PMDETA, Acros Organics, 98%), 2-bromoisobutyryl bromide (Alfa Aesar, 97%), and triethylamine (TEA, Beijing Chemical Reagent Co. Ltd., 99%) were all used as received. The tetrahydrofuran (THF) was purified by distillation over CaH_2. In order to remove copper (II), the copper (I) bromide (Shanghai Zhenxing Chemical Regent Factory, Shanghai, China) was stirred in glacial acetic acid, filtered, washed with ethanol three times, and then dried in vacuum. The toluene was distilled under reduced pressure. The cyclohexanone was dried with anhydrous magnesium sulfate and then filtered before use. The tertiary butyl acrylate (98%, Aldrich) (t-BuA) was distilled under reduced pressure before use. The trifluoroacetic acid, dimethyl sulfoxide (DMSO), anhydrous ethanol and disodium ethylene diamine tetraacetic acid (EDTA) were all used as received. The dodecyl-trimethylammonium bromide (C_{12}TAB, 99%, Shanghai Jingchun Reagent Co., China) was dried at 60 °C under vacuum before use. Double distilled water was used as the solvent.

2.2. Methods

^{1}H NMR spectra were recorded on a Varian INOVA 500 MHz spectrometer. The chemical shifts are given in parts per million (ppm). Tetramethyl silane (TMS) was used as the internal standard.

FT-IR spectra were recorded on a BIO-BAD EAALIBUR FTA-3000 Fourier transform infrared spectrometer. Transmittance measurements were taken on the samples in KBr pellets.

The conductivity measurements were performed with a DDS-11A conductivity meter equipped with platinized platinum electrodes (cell constant = 1.008 cm^{-1}). The meter was initially calibrated with a KCl standard solution. C_{12}TAB solutions with different concentration were put into a thermostated water bath at 25 °C during measurements.

The surface tension measurements of all the solutions were performed using the Wilhelmy plate method with a DCAT21 tensiometer (Germany) at 25 °C. The accuracy was 0.01 mN m^{-1}.

UV–vis spectra were obtained from a Purkinje General (China) T6 UV/Vis Spectrophotometer.

Transmission electron microscopy was conducted with a Philips T20ST electron microscope at an acceleration voltage of 200 kV. A small drop of micellar solution was deposited onto a preheated carbon-coated copper grid and dried at atmospheric pressure. Samples were also prepared by staining with phosphotungstic acid.

All samples were filtered through a 0.45 μm Millipore filter into clean scintillation vials and characterized by dynamic light scattering measurements performed on a Brookhaven BI-200SM goniometer, equipped with a digital correlator (BI-9000AT) at 532 nm.

2.3. Synthesis

2.3.1. Synthesis of macroinitiator (ECBr)

The macroinitiator for ATRP was synthesized by acrylation using 2-bromoisobutyryl bromide and EC according to the procedures in the literature (Kang et al., 2006). The grafting degree of Br can be controlled by changing the reaction time. EC (6.9 g, unit of glucose 30.0 mmol) was dissolved in a mixture of distilled THF (150 mL) and TEA (3.0 g, 30 mmol) in a 250 mL three-necked flask and the solution was stirred with a magnetic stirrer for 3.5 h. Then, 2-bromoisobutyryl bromide (20.8 g, 90.5 mmol) in 30 mL of distilled THF was added dropwise over the course of 2.5 h to the solution in an ice/water bath at 0 °C. The reaction mixture was then stirred at room temperature for 18 h. The resulting suspension was centrifuged and the clear upper solution was diluted with THF. The final solution was precipitated three times in distilled water. Finally, the product was freeze-dried. ^{1}H NMR spectra of EC and ECBr are shown in Fig. S1a and S1b in Supplementary information and by comparing the area of peak c (the methyl protons in the 2-bromoisobutyryl group) with that of peak a (the methyl protons in ethyl groups of EC), the degree of substitution of the 2-bromoisobutyryl group for the ECBr macroinitiator was determined to be 0.22.

The FT-IR spectra of pure EC and ECBr are shown in Fig. S2a and S2b, respectively in Supplementary information, the peak at about 1737 cm^{-1} in Fig. S2b can be ascribed to the ester bond of 2-bromoisobutyryl.

Furthermore, the ^{1}H NMR spectrum of ECBr in Fig. S1b reveals major peaks at 1.95 ppm (peak c) which is due to the methyl protons in the 2-bromoisobutyryl group and at 2.75–4.75 ppm (peak b) which is due to the methylene in the ethyl group and hydrogen protons in anhydroglucose unit. These results indicate that the synthesis of the macroinitiator was successful.

2.3.2. Synthesis of ethyl cellulose-g-poly tert-butyl acrylate (EC-g-PtBuA)

The EC-g-PtBuA was prepared according to a previously reported method (Kang et al., 2006). ECBr ($M_{w,unit}$ = 272.04, 1.3 g, the residual Br was 1.2 mmol) and, PMDETA (0.2 g, 1.2 mmol) were dissolved in deoxygenated toluene (13.3 g) and cyclohexanone (5.7 g) in a 50 mL flask with a magnetic stirrer. The flask was degassed by three freeze-evacuate-thaw cycles. Then t-BuA (29.5 g, 0.24 mol) and CuBr (0.2 g, 1.2 mmol) were added to the reaction system. The reaction mixture was degassed by three freeze-evacuate-thaw cycles. After all the reactants were dissolved,

the polymerization was performed at 80 °C for the required time. After being cooled to room temperature, the flask was exposed to air and the solvent was removed. The crude product was then dissolved in THF and precipitated three times in an aqueous solution of disodium EDTA to remove the catalyst. The product was obtained by freeze-drying. ^{1}H NMR spectrum of EC-g-PtBuA (Fig. S1c in Supplementary information) was taken and by comparing the area of peak f (methylene protons in the repeating unit of the grafted chains) with that of peak a (the methyl protons in ethyl groups of EC), the length of the grafted chain was determined to be 10.

The FT-IR spectrum of EC-g-PtBuA is shown in Fig. S2c in Supplementary information. The peak at about 1737 cm^{-1} is assigned to the stretching vibration of the carbonyl group.

The ^{1}H NMR spectrum of the EC-g-PtBuA is shown in Fig. S1c in Supplementary information. The peak at 1.15 ppm is assigned to the methyl protons of the ethyl group. The peaks at 2.25 and 1.84 ppm are respectively assigned to the methylene and methine protons in the repeating unit of the grafted chains and the peak at 1.27 ppm is assigned to the methyl protons of the tert-butyl group.

2.3.3. Synthesis of ethyl cellulose-g-sodium polyacrylate (EC-g-SPA)

According to the procedure in the literature (Kang et al., 2006), EC-g-PtBuA (3.8 g) was dissolved in anhydrous CH_2Cl_2 (200 mL). Trifluoroacetic acid (40 mL) was added and the mixture was stirred for 24 h. The obtained solid was dissolved in a small amount of DMSO. Then the solution was dialyzed (MWCO3500) against distilled water until the DMSO was removed. After the aqueous solution was neutralized, a white solid was obtained by freeze-drying.

The FT-IR spectrum for EC-g-SPA is shown in Fig. S2d in Supplementary information. The wide peak from 3700 to 2800 cm^{-1} can be assigned to the associating hydroxyls of the carboxyl groups.

Compared with the ^{1}H NMR spectrum for EC-g-PtBuA (Fig. S1c), the ^{1}H NMR spectrum for EC-g-SPA has no peak at 1.27 ppm (the methyl protons of the tert-butyl group) and there is a peak at 12.10 ppm (the proton of the carboxy group) (Fig. S1d in Supplementary information). These results confirm that the EC-g-SPA was successfully obtained.

2.4. Sample preparation

Before the C_{12}TAB and EC-g-SPA aqueous stock solutions were prepared, the C_{12}TAB and EC-g-SPA were dried in a vacuum oven at 60 °C for 48 h to remove absorbed water. All samples were prepared by dropping aqueous solutions of surfactant into polyelectrolyte solutions at the ratio needed to give the desired composition. The surfactant solution was slowly added to the EC-g-SPA solution using a constant-flow bump while the solution was gently stirred in order to avoid premature local precipitation. The final solutions were obtained by adding double distilled water. To ensure complete dissolution and equilibrium, the prepared solutions were kept at room temperature for 48 h before testing.

3. Results and discussion

3.1. The amphiphilic properties of EC-g-SPA

It is well known that amphiphilic polymers with a suitable hydrophilic/hydrophobic balance can form micellar structures when exposed to selective solvents. The amphiphilic EC-g-SPA chains, which consist of hydrophilic and hydrophobic segments, should form micelles in water. Fig. 1 shows the surface tension isotherm of EC-g-SPA versus its concentration. According to

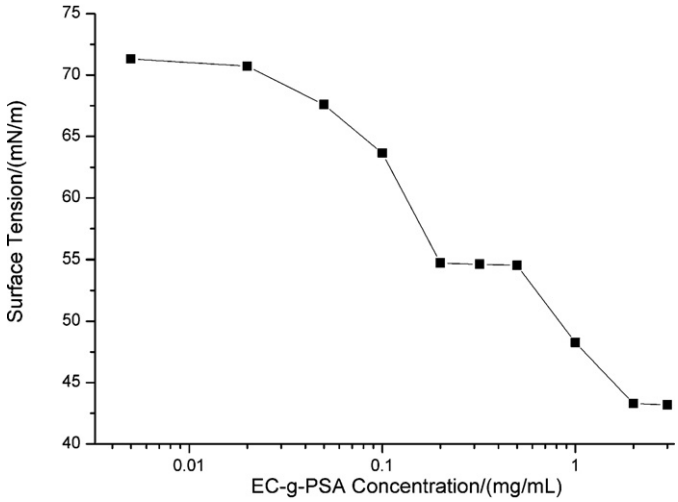

Fig. 1. Surface tension-EC-g-SPA concentration dependence for aqueous EC-g-SPA solutions.

Fig. 1, the surface tension (ST) decreased greatly in the concentration range from 0.005 to 0.2 wt%. From 0.2 to 0.5 wt%, the ST was fairly constant. Above concentration of 0.5 wt%, the ST decreased until a second plateau occurred from 2.0 to 3.0 wt%. According to the literature (Kang et al., 2006), in aqueous solutions and at a concentration of 1 mg/mL, the amphiphilic EC-g-SPA chains can self-assemble into both single-chain and multi-chains micelles. The concentration of the EC-g-SPA solutions in this work is higher than 1 mg/mL (0.2–0.5 wt%). So, we think that at concentrations of 0.2–0.5 wt%, EC-g-SPA self-assembles into multi-chains micelles by intermolecular interactions, which corresponds to the first surface tension plateau. The second plateau indicates that when the aqueous concentrations were 2.0–3.0 wt%, then the micelles composed of several EC-g-SPA chains aggregated into bigger particles through the hydrophobic effect. The behavior of the EC-g-SPA/C_{12}TAB complexes in the bulk and at the interface was influenced by the structure of the EC-g-SPA aggregate. The micellar structure was formed at the first plateau, so a concentration of 0.4 wt% was selected to complex the EC-g-SPA with C_{12}TAB.

3.2. Interfacial properties of the EC-g-SPA/C_{12}TAB complexes

A plot of surface tension as a function of C_{12}TAB concentration for EC-g-SPA/C_{12}TAB system is shown in Fig. 2(a). In addition the surface tension behavior of C_{12}TAB alone solutions is shown in Fig. 2(b) to compare to that of the EC-g-SPA/C_{12}TAB system. As shown in Fig. 2(b), there is a minimum surfactant tension at 14 mM and the surface tension reaches a relatively stable value at 16 mM corresponding to CMC. The concentration of 16 mM is referred to as CMC because trace amount of impurities in the C_{12}TAB leads to the appearance of the minimum at 14 mM in Fig. 2(b). To accurately determine the CMC of C_{12}TAB, conductivity measurements were done (inset in Fig. 2). As shown in the inset, the CMC of pure C_{12}TAB is 16 mM. Fig. 2(a) is similar to model plots for polymer/surfactants depicted by Goddard and Ananthapadmanabahn (1993). As shown in Fig. 2(a), there are three distinct points (T1, T2′ and T2) in the EC-g-SPA/C_{12}TAB surface tension plot. The first point, T1 (at 0.8 mM), corresponds to the concentration at which micellization of the C_{12}TAB monomers on the EC-g-SPA chains in the bulk solution begins. This concentration is denoted as the CAC for the EC-g-SPA/C_{12}TAB system. The second point, T2′ (at 4 mM), corresponds to the concentration at which the EC-g-SPA is saturated with the C_{12}TAB micelles. The third point is T2 (at 10 mM) and is where the second plateau in the surface tension is formed.

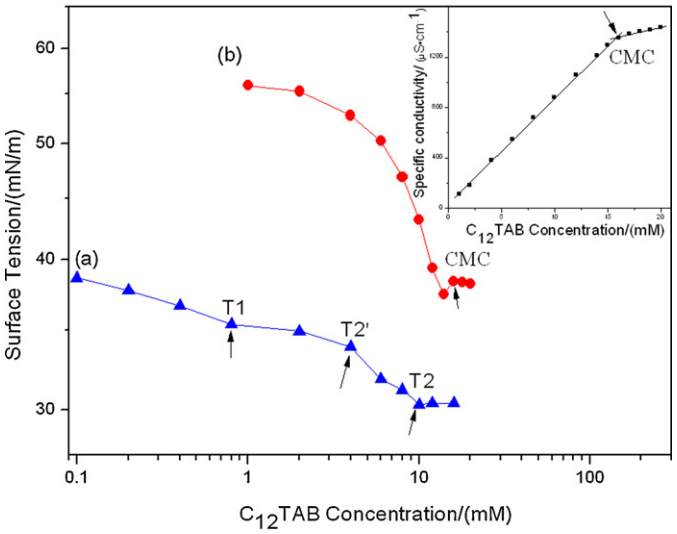

Fig. 2. Surface tension-C_{12}TAB concentration dependence for aqueous solutions of EC-g-SPA/C_{12}TAB mixture. The EC-g-SPA concentrations are: (a) 0.4 wt%, and (b) 0 wt%. Inset: specific conductivity-C_{12}TAB concentration curve of C_{12}TAB.

Beyond this point, further addition of C_{12}TAB leads to the formation of free micelles of C_{12}TAB in the bulk solution.

But there are two aspects regarding Fig. 2(a). One is that there is no surface tension hump in Fig. 2(a) which was seen in the polyDMDAAC/SDS curves (Staples, Tuchker, Penfold, Warren, & Thomas, 2002; Staples, Tuchker, Penfold, Warren, Thomas, & Taylor, 2002) and the NaPSS/C_nTAB (n = 14, 16) curves (Taylor et al., 2003). The presence of hump may be attributed to the competitive formation of a surface-active complexes consisting of surfactant monomers bound to the polymer backbone (P_S), a surface-active polymer–surfactant complexes containing a bilayer or a layer of micelles, which binds onto the underside of the P_S complexes (P'_S) and a non-surface-active polymer-micellar aggregate where surfactant molecules cooperatively absorb to the polymer backbone in the form of micelles to form a necklace-like structure (P_{Sm}) (Bell et al., 2007). The hump in the surface tension curves disappears if P'_S is more stable than P_{Sm}, which suggests P'_S is favorably formed. This is also the case for the present EC-g-SPA/C_{12}TAB system. Another reason for the hump absence may be that, as the EC-g-SPA is amphiphilic, its complexes with the cationic surfactant may be also adsorbed at the air/solution interface. The other aspect, which has also been seen in the literature (Taylor & Thomas, 2002a), is that the T2 is lower than the CMC of the pure C_{12}TAB, in contrast to the behavior for weakly interacting systems where this concentration is generally higher than the CMC of pure C_{12}TAB. This may be attributed that there is strong synergy between amphiphilic EC-g-SPA and C_{12}TAB at the air/solution interface, which causes the adsorption of the EC-g-SPA/C_{12}TAB complexes at lower surfactant concentrations than in the pure surfactant (Taylor & Thomas, 2002b).

3.3. The diameter distribution and morphology of the complexes

Fig. 3 shows the size distribution of 0.4 wt% EC-g-SPA/C_{12}TAB complexes at different surfactant concentrations. To better interpret Fig. 3, the curves were transformed into a curve of hydrodynamic diameter (D_h) as a function of the C_{12}TAB concentration and this is shown in Fig. 4. At concentration of 0.4 wt% EC-g-SPA self-assembles into multi-chains micelles (Scheme 1(a)) (Kang et al., 2006). Pictures of the EC-g-SPA/C_{12}TAB solutions at different surfactant concentrations are shown in Fig. 5. There is a correlation between the microscopic binding interactions and

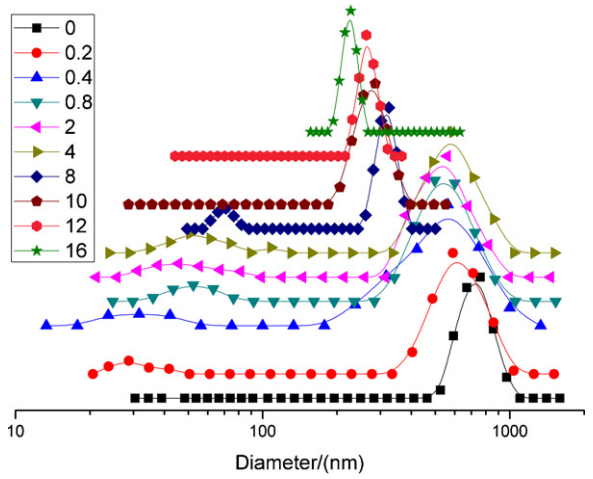

Fig. 3. Size distributions of EC-g-SPA/C_{12}TAB complexes at different C_{12}TAB concentration.

the macroscopic phenomenon, which can be seen by comparing Figs. 4 and 5. As one may observe from the figures, D_h decreased slightly and the solutions are transparent (Fig. 5(a)) till a C_{12}TAB concentration of 0.8 mM, which is the CAC. The CAC determined from surface tension and DLS measurements is the same (see Figs. 2(a) and 4). The decrease in D_h is due to the electrostatic binding of the C_{12}TAB monomers to the carboxylate groups on the EC-g-SPA backbones, which shields the electrostatic repulsions between the grafted side chains, causing the shrinking of polymer chains. When the C_{12}TAB concentration is increased from 0.8 mM to 4 mM, an increase in D_h occurs and the solutions become turbid (Fig. 5(b)). These are attributed to the polyelectrolyte/surfactant complexation, induced by the micellization of the surfactant monomers that are electrostatically bound to the carboxylate groups of EC-g-SPA. As the C_{12}TAB concentration is increased above 4 mM, the D_h decreased sharply and the solution gradually turned opaque (Fig. 5(d)–(f)). This may be due to the dissociation of EC-g-SPA multi-chains micelles bound with C_{12}TAB micelles, which greatly increases the number of single EC-g-SPA chains bound with C_{12}TAB micelles in the solution and in turn the D_h of EC-g-SPA/C_{12}TAB complexes decreases (Wang & Tam, 2005). As shown in Table 1, the turbidity of the complex solutions increased as the surfactant concentration rises. This may be attributed that being

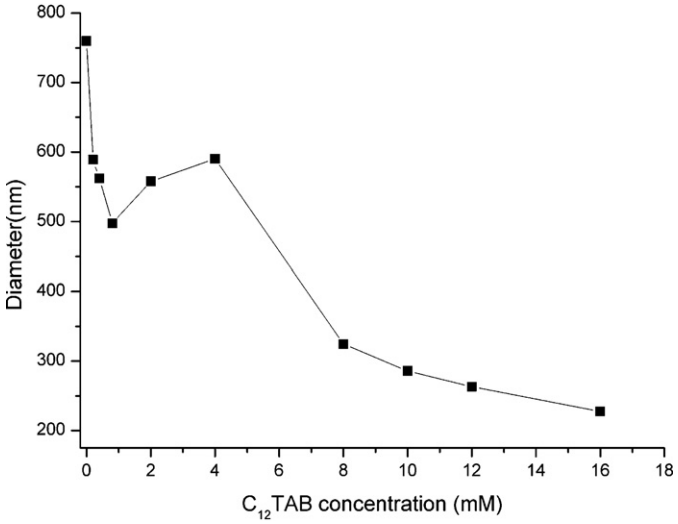

Fig. 4. The hydrodynamic diameters of EC-g-SPA/C_{12}TAB at different C_{12}TAB concentration.

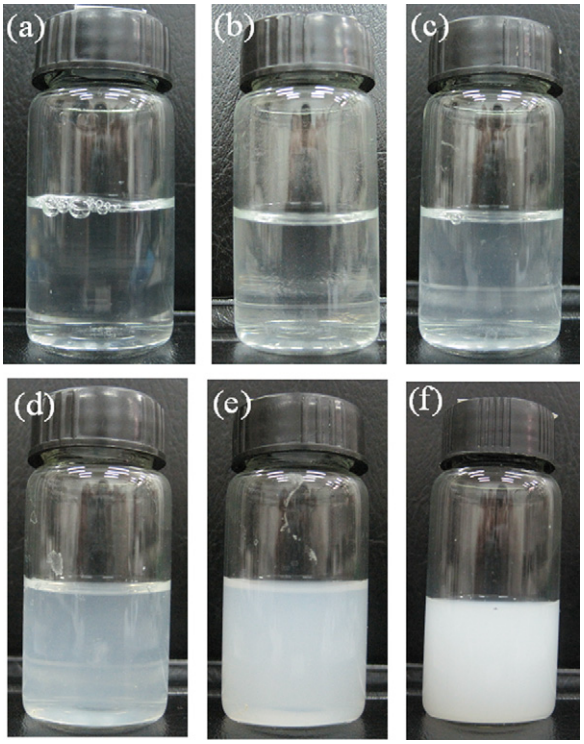

Fig. 5. Pictures of EC-g-SPA/C_{12}TAB at different C_{12}TAB concentrations: (a) 0.2 mM, (b) 0.8 mM, (c) 4 mM, (d) 8 mM, (e) 10 mM and (f) 16 mM.

Table 1
Turbidity of the complex solutions.

[C_{12}TAB] (mM)	100 − % transmittance
0	0
0.2	0.5
0.4	0.7
0.8	2
2	4
4	5.7
8	38.9
10	74.8
12	89.9
16	98.2

single-chain copolymer micelles, the surfactant binding leads to faster charge neutralization. After sitting for months, all solutions were still stable, which suggests that the comb polyelectrolyte does not undergo phase separations.

TEM images of the 0.4 wt% EC-g-SPA solutions with different surfactant concentration were used to identify the microstructures of the formed complexes. As the surfactant concentration (Cs) is increased, a variety of inhomogeneous structures appeared in the solutions. As shown in Fig. 6a, the micellar structure of 0.4 wt% EC-g-SPA is globular. Fig. 6b shows the TEM image of the complex solution at Cs = 4 mM. Typically, there are two kinds of spherical aggregates with diameters of approximately 100 and 300 nm. This concentration is well above the CAC, so the large aggregates are the cluster of some EC-g-SPA chains whereas the small particles are the EC-g-SPA/C_{12}TAB complexes. At Cs = 8 mM (Fig. 6c), the TEM images indicate that there are some aggregates with different structure compared with the structure shown in Fig. 6b, which indicates that the structural transformation of EC-g-SPA chains is induced by the complexation when the C_{12}TAB is higher than 4 mM. Fig. 6d shows the TEM image at Cs = 10 mM and there is an indication that a well-ordered necklace of beads is formed (Kong, Cao, & Hai, 2007). A well-ordered necklace is probably formed from spherical surfactant micelles wrapped by polymer chains. The surface tension at this concentration (T2) is at the onset of the second plateau. As discussed above, attention must be paid to that, during the increase of Cs, the different structures of aggregates are formed in the EC-g-SPA/C_{12}TAB complexes system. These results are consistent with the ones obtained from DLS. The diameters obtained from the TEM images are much less than those obtained from DLS measurements. This is because the diameter obtained from DLS is hydrodynamic diameter. TEM images for the other concentrations of surfactant were not obtained because electrons did not transmit through these samples. Obviously, an increase in Cs leads to a change in the size and shape of the aggregates.

Scheme 1 illustrates the structure evolution for the EC-g-SPA/C_{12}TAB complexes as increasing amounts of C_{12}TAB are added to the EC-g-SPA solution. As shown in Scheme 1b, several EC-g-SPA chains self-assemble into globular micelles in the free-C_{12}TAB solution. The EC-g-SPA chains are stretched because of repulsive interactions between the grafted chains. Once C_{12}TAB is added, the monomers of C_{12}TAB are bound to the carboxylate groups of the grafted chains and polyelectrolyte/surfactant complexes are

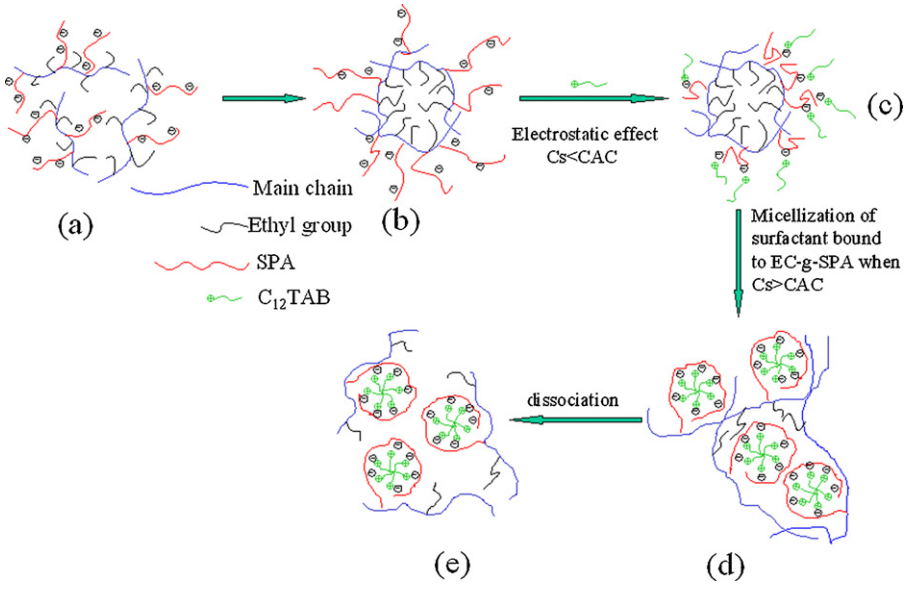

Scheme 1. Structure evolution of the EC-g-SPA/C_{12}TAB complexes as increasing amounts of C_{12}TAB are added to the EC-g-SPA solution.

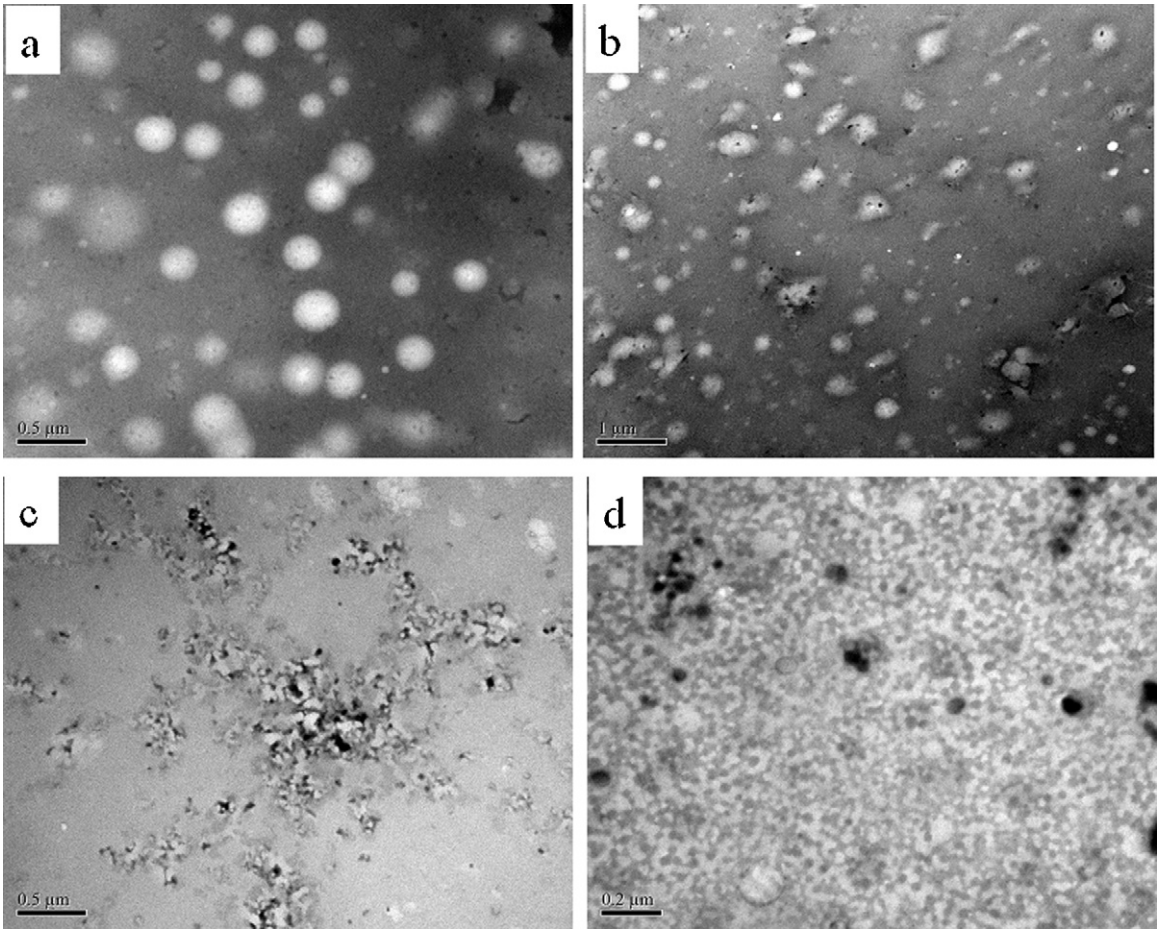

Fig. 6. TEM images for 0.4% EC-g-PSA/C_{12}TAB complexes at various surfactant concentrations: (a) 0 mM, (b) 4 mM, (c) 8 mM, and (d) 10 mM.

formed (Ruckenstein, Huber, & Hoffmann, 1987), which weakens the electrostatic repulsions between the grafted chains. Hence, the EC-g-SPA clusters shrink (Scheme 1(c)), with corresponding decrease in D_h. The surfactant molecules that are electrostatically bound to the grafted chains of the EC-g-SPA start to form micelles (Scheme 1(d)) at the CAC (0.8 mM). An increase in the D_h of the EC-g-SPA/C_{12}TAB occurs when the C_{12}TAB concentration is increased from 0.8 mM to 4 mM. This may be attributed to the C_{12}TAB micellization on the multi-chain EC-g-SPA aggregates, which is going on till a surfactant concentration of 4 mM, when the EC-g-SPA is saturated with the C_{12}TAB micelles. The D_h of the complexes decreases when the C_{12}TAB concentration is higher than 4 mM. This may be due to the dissociation of multi-chain EC-g-SPA micelles bound with C_{12}TAB micelles, which greatly increases the number of single EC-g-SPA chains in the solution and in turn the D_h of EC-g-SPA/C_{12}TAB complexes decreases (Scheme 1(e)) (Wang & Tam, 2005). After the dissociation, the structure of complex could be depicted as a "necklace", in which the C_{12}TAB micelles are "beads" and the EC-g-SPA chains are the "strings" that attach the "beads".

4. Conclusions

A comb polyelectrolyte EC-g-SPA was synthesized by ATRP. Various structured EC-g-SPA aggregates were formed in aqueous solution of different concentration. Interactions between the anionic amphiphilic EC-g-SPA and C_{12}TAB were investigated by surface tension, turbidity, DLS and TEM. The CAC of the 0.4 wt% EC-g-SPA/C_{12}TAB system was 0.8 mM. When the C_{12}TAB concentration was lower than CAC, the D_h of the complexes decreased as the surfactant concentration increased. However, when the C_{12}TAB concentration was increased above the CAC, the D_h of the complexes initially increased slightly and then, decreased sharply as the C_{12}TAB concentration was further increased. These results indicate that the structural transformation of EC-g-SPA chains is induced by the complexation. The TEM images showed that there are different structures of complexes at different C_{12}TAB concentration. The evolution of the interactions and the structure of the EC-g-SPA/C_{12}TAB system as a function of C_{12}TAB concentration were also discussed.

Acknowledgements

This work was supported by the National Natural Science Foundation of China (20804027, 21074088) and the Youth Development Foundation of Tianjin Agriculture College (2007007).

Appendix A. Supplementary data

Supplementary data associated with this article can be found, in the online version, at http://dx.doi.org/10.1016/j.carbpol.2012.04.032.

References

Bell, C. G., Breward, C. J. W., Howell, P. D., Penfold, J., & Thomas, R. K. (2007). Macroscopic modeling of the surface tension of polymer–surfactant systems. *Langmuir*, *23*, 6042–6052.

Cui, T. Y., Cui, F., Zhang, J. H., Wang, J. Y., Huang, J., Lü, C. L., et al. (2006). From monomeric nanofibers to PbS nanoparticles/polymer composite nanofibers through the combined use of γ-irradiation and gas/solid reaction. *Journal of the American Chemical Society*, *128*, 6298–6299.

Fundin, J., Hansson, P., Brown, W., & Lidegran, I. (1997). Poly(acrylic acid)-cetyltrimethylammonium bromide interactions studied using dynamic and static light scattering and time-resolved fluorescence quenching. *Macromolecules*, *30*, 1118–1126.

Goddard, E. D. (1986). Polymer–surfactant interaction. Part I. Uncharged water-soluble polymers and charged surfactants. *Colloids and Surface*, *19*, 255–301.

Goddard, E. D. (2002). Polymer/surfactant interaction: Interfacial aspects. *Journal of Colloid and Interface Science*, *256*, 228–235.

Goddard, E. D., & Ananthapadmanabahn, K. P. (1993). *Interactions of surfactants with polymers and proteins*. CPC Press: Boca Raton.

Hansson, P., & Almgren, M. (1994). Interaction of alkyltrimethylammonium surfactants with polyacrylate and poly(styrenesulfonate) in aqueous solution: Phase behavior and surfactant aggregation numbers. *Langmuir*, *10*, 2115–2124.

Jones, M. N. (1967). The interaction of sodium dodecyl sulfate with polyethylene oxide. *Journal of Colloid and Interface Science*, *23*, 36–42.

Jönsson, B., Lindman, B., Holmberg, K., & Kronberg, B. (1998). *Surfactant and polymers in aqueous solution*. John Wiley & Sons.

Kang, H. L., Liu, W. Y., He, B. Q., Shen, D. W., Ma, L., & Huang, Y. (2006). Synthesis of amphiphilic ethyl cellulose grafting poly(acrylic acid) copolymers and their self-assembly morpholofies in water. *Polymer*, *47*, 7927–7934.

Kong, L. J., Cao, M., & Hai, M. T. (2007). Investigation on the interaction between sodium dodecyl sulfate and cationic polymer by dynamic light scattering, rheological, and conductivity measurements. *Journal of Chemical & Engineering Data*, *52*(3), 721–726.

Li, X. B., Lin, Z. C., Cai, J., Scriven, L. E., & Davis, H. T. (1995). Polymer-induced microstructural transitions in surfactant solutions. *Journal of Physical Chemistry*, *99*, 10865–10878.

Lee, J., & Moroi, Y. (2004). Investigation of the interaction between sodium dodecyl sulfate and cationic polymers. *Langmuir*, *20*, 4376–4379.

Middleton, R., English, R. J., Williams, P. A., & Broze, G. (2005). Interaction of sodium dodecyl sulfate with methacrylate-PEG comb copolymers. *Langumir*, *21*, 5174–5178.

Miyake, M., & Kakizawa, Y. (2002). Study on the interaction between polyelectrolytes and oppositely charged ionic surfactants. Solubilized state of the complexes in the postprecipitation region. *Colloid & Polymer Science*, *280*, 18–23.

Pakula, T., Zhang, Y., Matyjaszewski, K., Lee, H., Boerner, H., Qin, S. H., et al. (2006). Molecular brushes as super-soft elastomers. *Polymer*, *47*, 7198–7206.

Penfold, J., Tucher, I., Thomas, R. K., Taylor, D. J. F., Zhang, X. L., Bell, L., et al. (2007). The interaction between sodium alkyl sulfate surfactants and the oppositely charged polyelectrolyte, polyDMDAAC, at air–water interface: The role of alkyl chain length and electrolyte and comparison with theoretical predictions. *Langmuir*, *23*, 3128–3136.

Rodríguez, R., Alvarez-Lorenzo, C., & Concheiro, A. (2003). Influence of cationic cellulose structure on its interactions with sodium dodecylsulfate: Implications on the properties of the aqueous dispersions and hydrogels. *European Journal of Pharmaceutics and Biopharmaceutics*, *56*, 133–142.

Ruckenstein, E., Huber, G., & Hoffmann, H. (1987). Surfactant aggregation in the presence of polymers. *Langmuir*, *3*(3), 382–387.

Staples, E., Tuchker, I., Penfold, J., Warren, N., & Thomas, R. K. (2002). Organization of polymer–surfactant mixtures at the air–water interface: Poly(dimethyldiallylammonium chloride), sodium dodecyl sulfate, and hexaethylene glycol monododecyl ether. *Langmuir*, *18*, 5139–5146.

Staples, E., Tuchker, I., Penfold, J., Warren, N., Thomas, R. K., & Taylor, D. J. F. (2002). Organization of polymer–surfactant mixtures at the air–water sodium dodecyl sulfate interface: Poly(dimethyldiallylammonium chloride). *Langmuir*, *18*, 5147–5153.

Silvério, C. A., & Okano, L. T. (2004). Laser flash photolysis and time-resolved fluorescence measurement of the aggregation number of SDS-biopolymer complexes. *Colloids and Surfaces B: Biointerfaces*, *38*, 41–46.

Svensson, A., Sjöström, J., Scheel, T., & Piculell, L. (2003). Phase and structures of a polyion-surfactant ion complex salt in aqueous mixtures: Cationic hydroxyethyl cellulose with dodecylsulfate counterions. *Colloid and Surfaces A: Physicochemical and Engineering Aspects*, *228*, 91–106.

Taylor, D. J. F., & Thomas, R. K. (2002a). The adsorption of oppositely charged polyelectrolyte/surfactant mixtures: Neutron reflection from dodecyl trimethylammonium bromide and sodium poly(styrene sulfonate) at the air/water interface. *Langmuir*, *18*, 4748–4757.

Taylor, D. J. F., & Thomas, R. K. (2002b). The adsorption of oppositely charged polyelectrolyte/surfactant mixtures at the air/water interface: Neutron reflection from dodecyl trimethylammonium bromide/sodium poly(styrene sulfonate) and sodium dodecyl sulfate/poly(vinyl pyridinium chloride). *Langmuir*, *18*, 9783–9791.

Taylor, D. J. F., Thomas, R. K., & Li, P. X. (2003). The adsorption of oppositely charged polyelectrolyte/surfactant mixtures. Neutron reflection from alkyl trimethylammonium bromides and sodium poly(styrene sulfonate) at the air/water interface: The effect surfactant chain length. *Langmuir*, *19*, 3712–3719.

Taylor, D. J. F., Thomas, R. K., & Penfold, J. (2007). Polymer/surfactant interactions at the air/water interface. *Advances in Colloid and Interface Science*, *132*, 69–110.

Trabelsi, S., Raspaud, E., & Langevin, D. (2007). Aggregate formation in aqueous solutions of carboxymethylcellulose and cationic surfactant. *Langmuir*, *23*, 10053–10062.

Varga, I., Mészáros, R., Makuška, R., Claesson, P. M., & Gilányi, T. (2009). Effect of graft density on the nonionic bottle brush polymer/surfactant interaction. *Langmuir*, *25*, 11383–11389.

Wang, C., & Tam, K. C. (2002). New insights on the interaction mechanism within oppositely charged polymer/surfactant systems. *Langmuir*, *18*, 6484–6490.

Wang, C., & Tam, K. C. (2005). Interactions between poly(acrylic acid) and sodium dodecyl sulfate: Isothermal titration calorimetric and surfactant ion-selective electrode studies. *Journal of Physical Chemistry B*, *109*, 5156–5161.

Wu, Q., Du, M., Shangguan, Y. G., Zhou, J. P., & Zheng, Q. (2009). Investigation on the interaction between C_{16}TAB and NaCMC in semidilute aqueous solution based on rheological measurement. *Colloids and Surfaces A: Physicochemical and Engineering Aspects*, *332*, 13–18.

Wu, Q., Shangguan, Y. G., Du, M., Zhou, J. P., Song, Y. H., & Zheng, Q. (2009). Steady and dynamic rheological behaviors of sodium carboxymethyl cellulose entangled semi-dilute solution with opposite charged surfactant dodecyltrimethylammonium bromide. *Journal of Colloid and Interface Science*, *339*, 236–242.

Zhang, M. F., Estournès, C., Bietsch, W., & Müller, A. H. E. (2004). Superparamagnetic hybrid nanocylinders. *Advanced Functional Materials*, *14*, 871–882.